Synthesis, Characterization and Biological Activity of Bis[3-ethyl-4-aryl-5-(2-methoxypyridin-5-yl)-1-propyl-1,3-dihydro-2*H*-imidazol-2-ylidene]gold(I) Complexes

Supplementary Information

Caroline Marie Gallati,[a‡] Sina Katharina Goetzfried,[a‡] Anna Ortmeier,[a,b,c] Jessica Sagasser,[a] Klaus Wurst,[d] Martin Hermann,[e] Daniel Baecker,[a,b] Brigitte Kircher,[b,c] and Ronald Gust*[a]

[a] Dr. C. M. Gallati, Dr. S. K. Goetzfried, Mag. A. Ortmeier, Mag. J. Sagasser, Dr. D. Baecker, Univ.-Prof. Dr. R. Gust*
Department of Pharmaceutical Chemistry, Institute of Pharmacy, Center for Molecular Biosciences Innsbruck, University of Innsbruck, Innrain 80/82, 6020 Innsbruck, Austria
* Corresponding author: E-mail: ronald.gust@uibk.ac.at
[b] Mag. A. Ortmeier, Dr. D. Baecker, Assoz.-Prof. Mag. Dr. B. Kircher
Tyrolean Cancer Research Institute, Innrain 66, 6020 Innsbruck, Austria
[c] Mag. A. Ortmeier, Assoz.-Prof. Mag. Dr. B. Kircher
Immunobiology and Stem Cell Laboratory, Department of Internal Medicine V (Hematology and Oncology), Medical University Innsbruck, Anichstraße 35, 6020 Innsbruck, Austria
[d] Ass.-Prof. Dr. K. Wurst
Institute for General, Inorganic and Theoretical Chemistry, University of Innsbruck, Innrain 80/82, 6020 Innsbruck, Austria
[e] Dr. M. Hermann
Department of Anesthesiology and Critical Care Medicine, Medical University Innsbruck, Anichstraße 35, 6020 Innsbruck, Austria

Table of Content

1. Analytical Characterization

1.1 ^{1}H NMR Spectroscopy

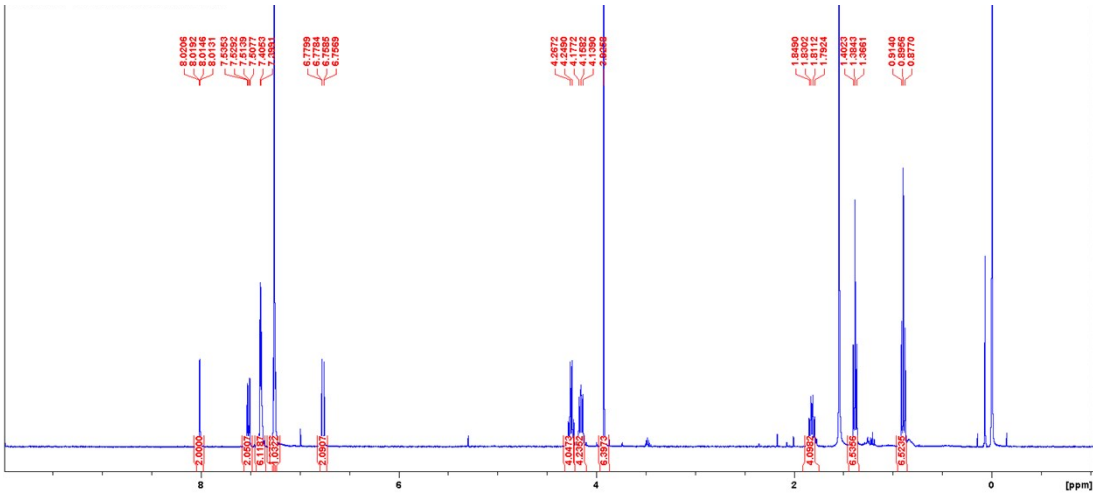

Figure S1. ^{1}H NMR spectrum of bis[3-ethyl-4-phenyl-5-(2-methoxypyridin-5-yl)-1-propyl-1,3-dihydro-2*H*-imidazol-2-ylidene]gold(I) bromide complex **2a** recorded in $CDCl_3$.

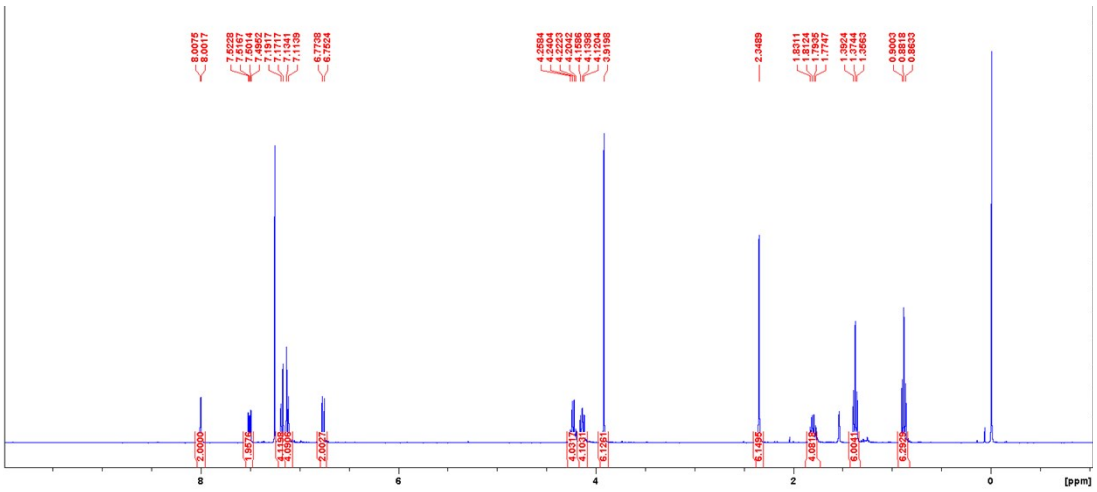

Figure S2. ^{1}H NMR spectrum of bis[3-ethyl-4-(4-methylphenyl)-5-(2-methoxypyridin-5-yl)-1-propyl-1,3-dihydro-2*H*-imidazol-2-ylidene]gold(I) bromide complex **2b** recorded in $CDCl_3$.

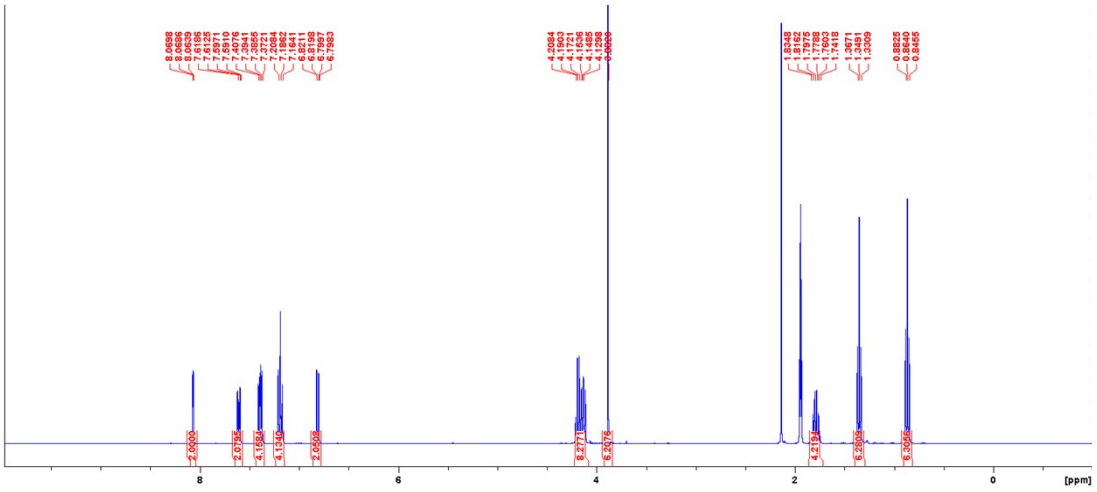

Figure S3. ^{1}H NMR spectrum of bis[3-ethyl-4-(4-fluorophenyl)-5-(2-methoxypyridin-5-yl)-1-propyl-1,3-dihydro-2*H*-imidazol-2-ylidene]gold(I) bromide complex **2c** recorded in CD_3CN.

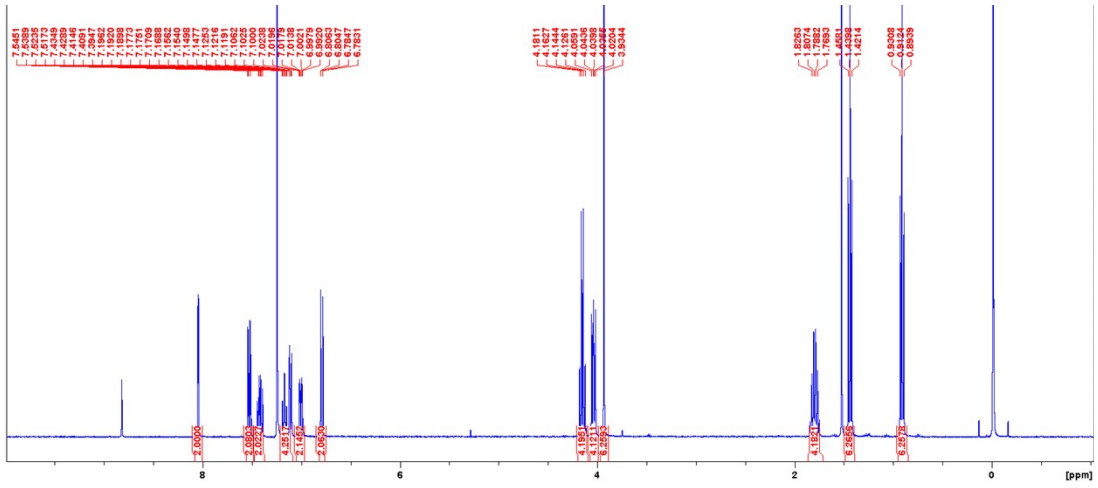

Figure S4. ^{1}H NMR spectrum of bis[3-ethyl-4-(3-fluorophenyl)-5-(2-methoxypyridin-5-yl)-1-propyl-1,3-dihydro-2*H*-imidazol-2-ylidene]gold(I) bromide complex **2d** recorded in $CDCl_3$.

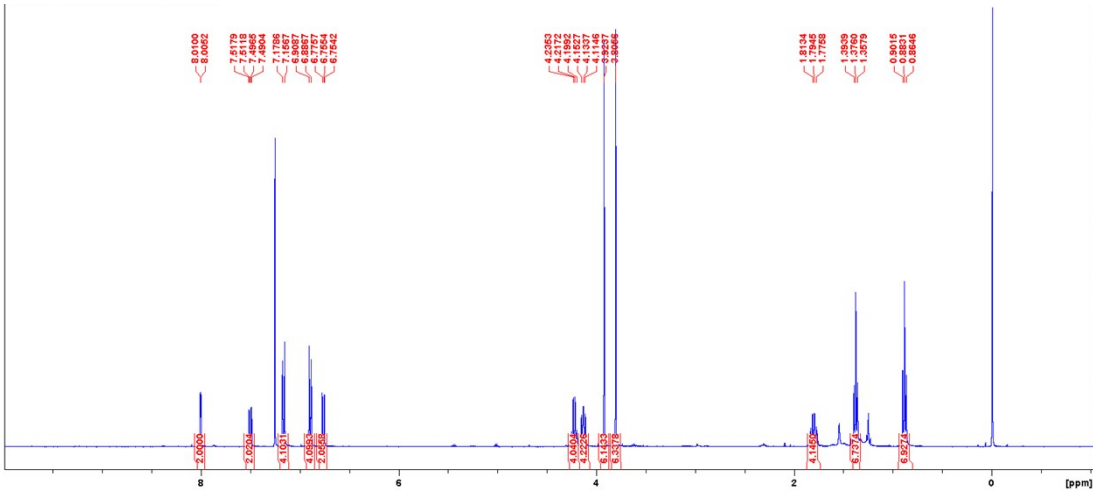

Figure S5. ^{1}H NMR spectrum of bis[3-ethyl-4-(4-methoxyphenyl)-5-(2-methoxypyridin-5-yl)-1-propyl-1,3-dihydro-2*H*-imidazol-2-ylidene]gold(I) bromide complex **2e** recorded in $CDCl_3$.

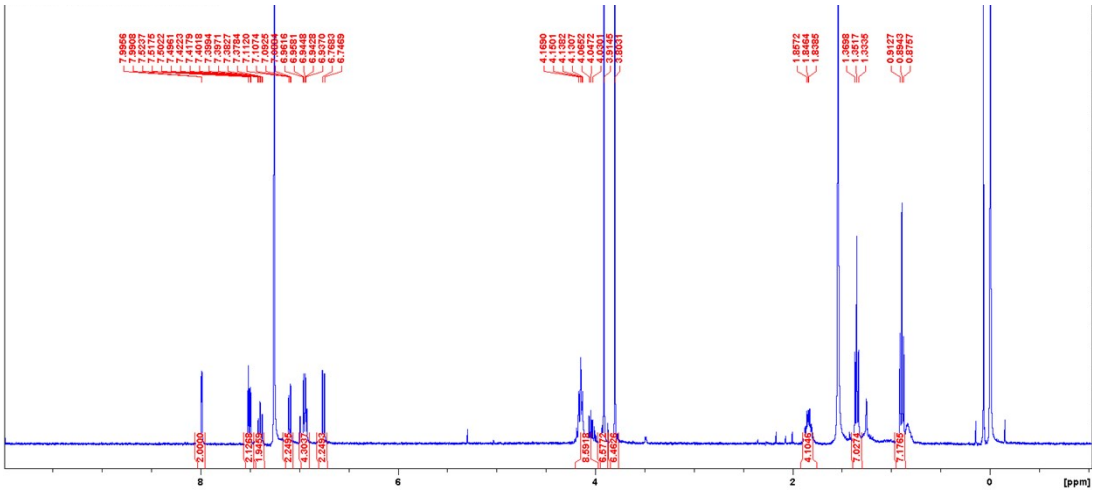

Figure S6. ^{1}H NMR spectrum of bis[3-ethyl-4-(2-methoxyphenyl)-5-(2-methoxypyridin-5-yl)-1-propyl-1,3-dihydro-2*H*-imidazol-2-ylidene]gold(I) bromide complex **2f** recorded in $CDCl_3$.

1.2 ^{13}C NMR Spectroscopy

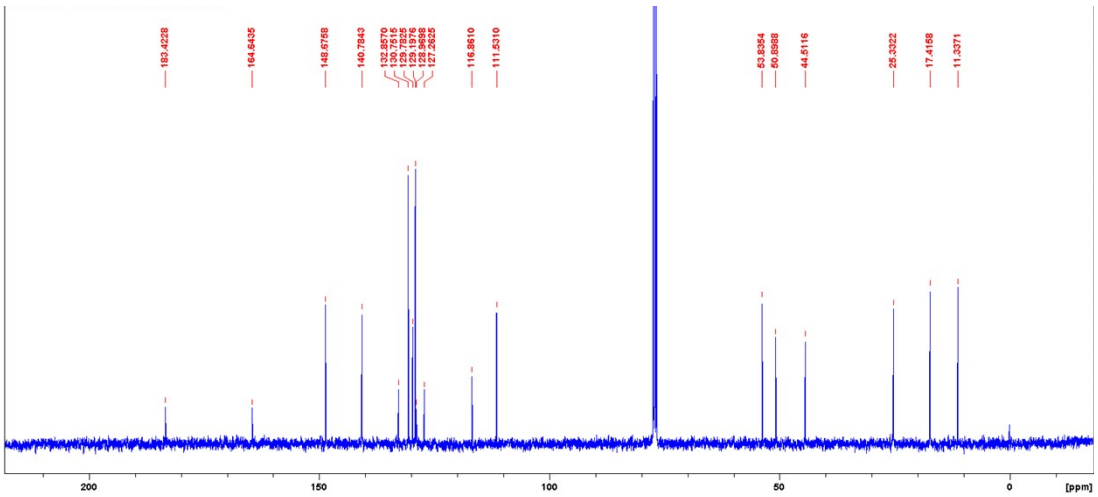

Figure S7. ^{13}C NMR spectrum of bis[3-ethyl-4-phenyl-5-(2-methoxypyridin-5-yl)-1-propyl-1,3-dihydro-2*H*-imidazol-2-ylidene]gold(I) bromide complex **2a** in $CDCl_3$.

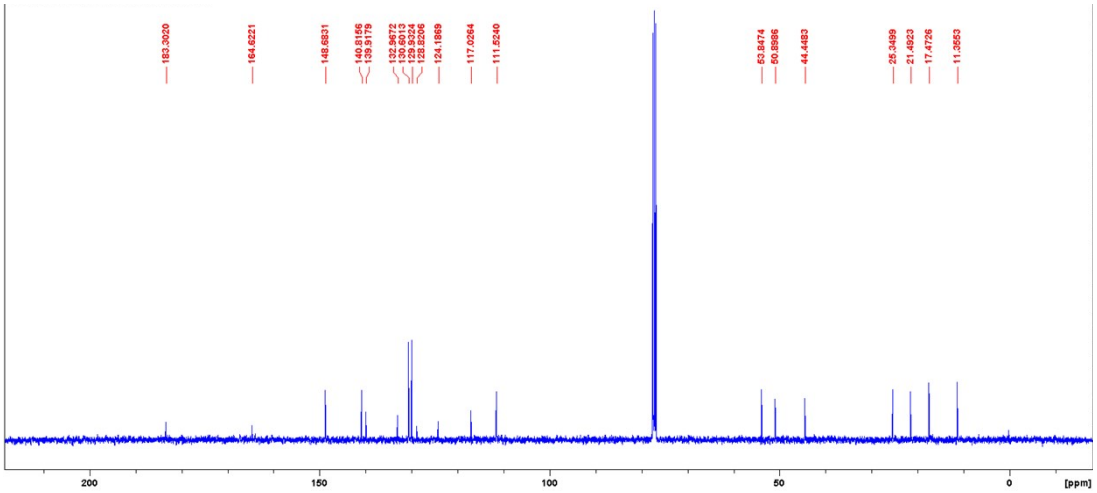

Fig. S8. ^{13}C NMR spectrum of bis[3-ethyl-4-(4-methylphenyl)-5-(2-methoxypyridin-5-yl)-1-propyl-1,3-dihydro-2*H*-imidazol-2-ylidene]gold(I) bromide complex **2b** in $CDCl_3$.

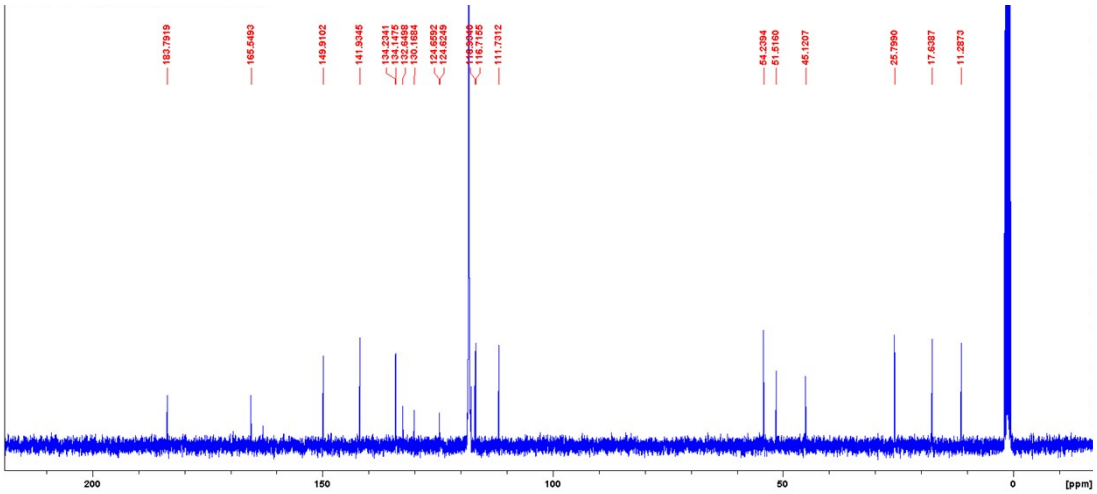

Figure S9. ^{13}C NMR spectrum of bis[3-ethyl-4-(4-fluorophenyl)-5-(2-methoxypyridin-5-yl)-1-propyl-1,3-dihydro-2*H*-imidazol-2-ylidene]gold(I) bromide complex **2c** in CD_3CN.

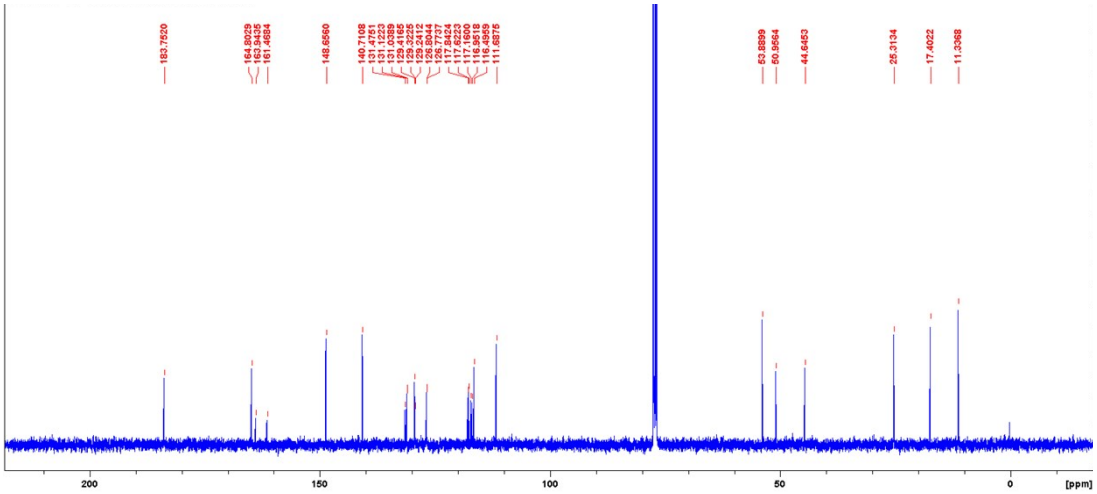

Figure S10. ^{13}C NMR spectrum of bis[3-ethyl-4-(3-fluorophenyl)-5-(2-methoxypyridin-5-yl)-1-propyl-1,3-dihydro-2*H*-imidazol-2-ylidene]gold(I) bromide complex **2d** in $CDCl_3$.

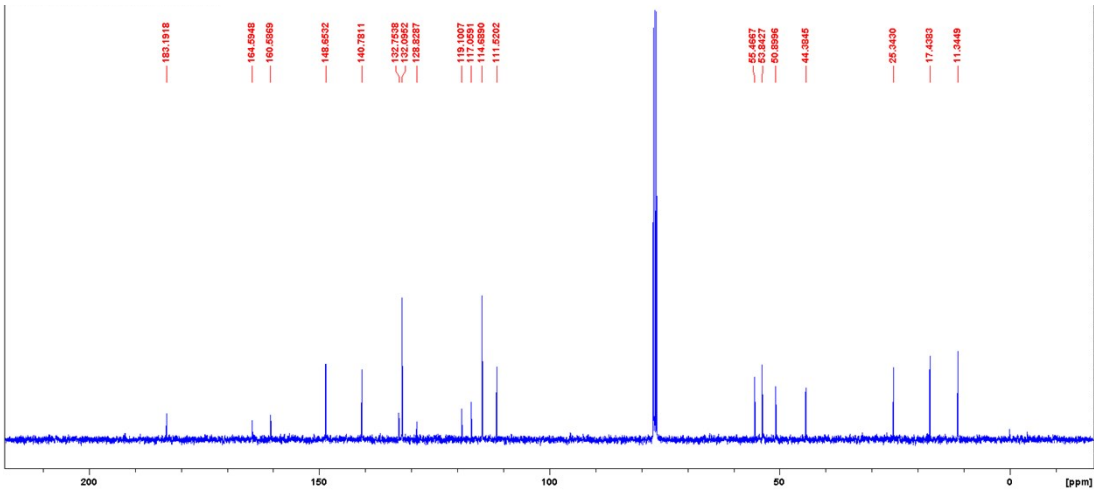

Figure S11. ^{13}C NMR spectrum of bis[3-ethyl-4-(4-methoxyphenyl)-5-(2-methoxypyridin-5-yl)-1-propyl-1,3-dihydro-2*H*-imidazol-2-ylidene]gold(I) bromide complex **2e** in $CDCl_3$.

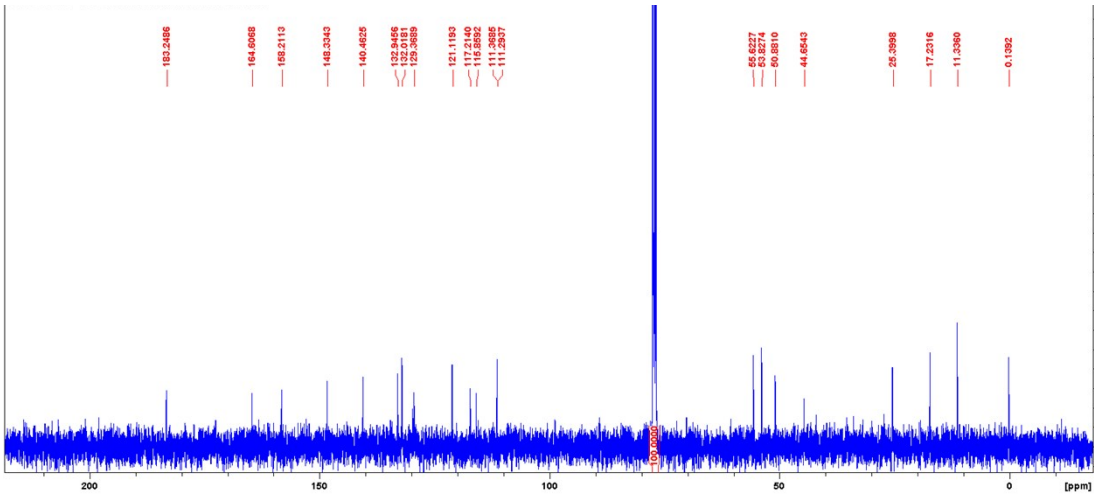

Figure S12. ^{13}C NMR spectrum of bis[3-ethyl-4-(2-methoxyphenyl)-5-(2-methoxypyridin-5-yl)-1-propyl-1,3-dihydro-2*H*-imidazol-2-ylidene]gold(I) bromide complex **2f** in $CDCl_3$.

1.3 UV-Vis Spectroscopy

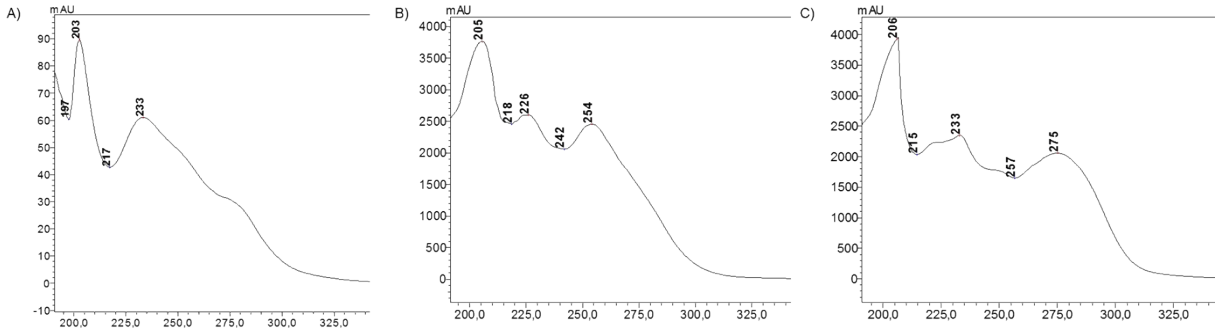

Figure S13. UV-Vis spectra of the NHC precursor **1e** (A), mono-NHC gold(I) complex **3e** (B) and bis-NHC gold(I) complex **2e** (C).

1.4 HR-MS Spectrometry

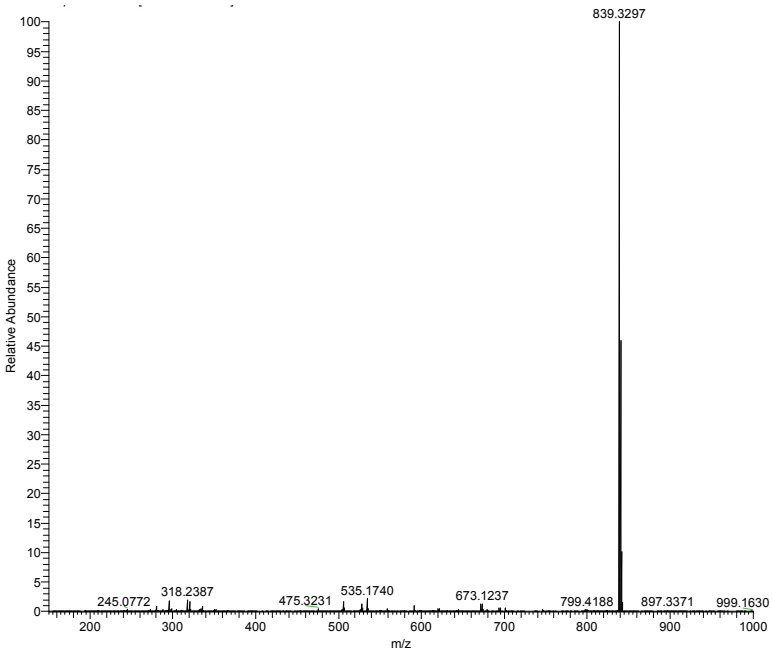

Figure S14. ESI-MS spectrum of **2a** (m/z 839).

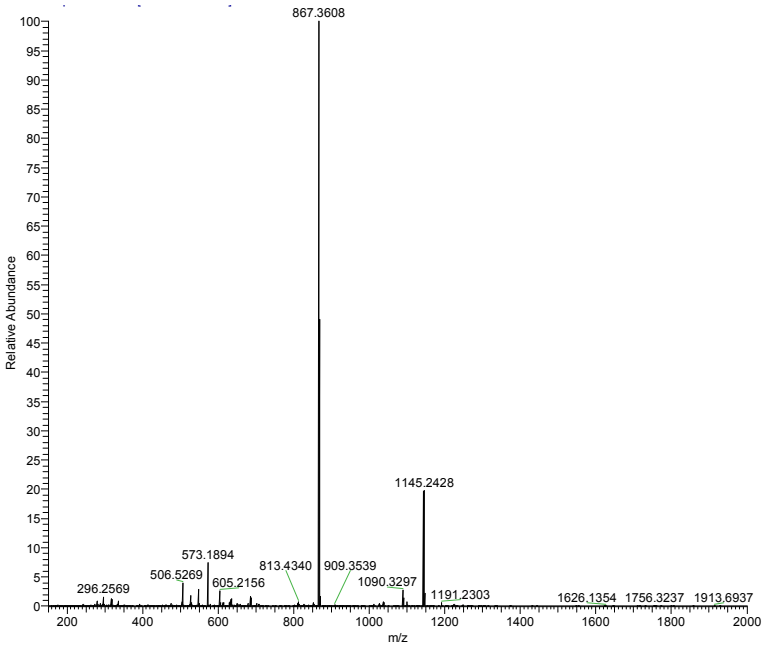

Figure S15. ESI-MS spectrum of **2b** (m/z 867). M/z 1145 corresponds to the $(NHC)_2Au_2Br$ species.

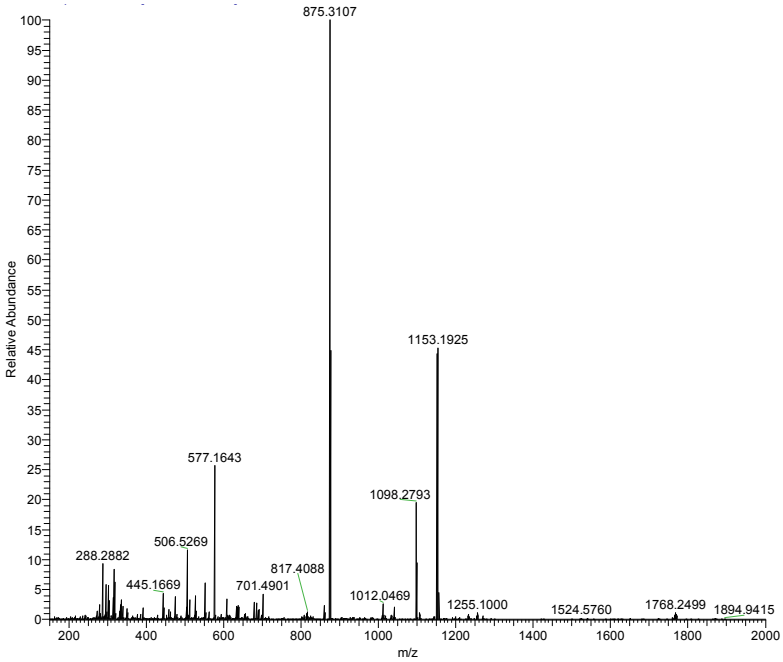

Figure S16. ESI-MS spectrum of **2c** (m/z 875). M/z 1153 corresponds to the $(NHC)_2Au_2Br$ species and m/z 1098 to the $(NHC)_2Au(III)Br_2$ complex.

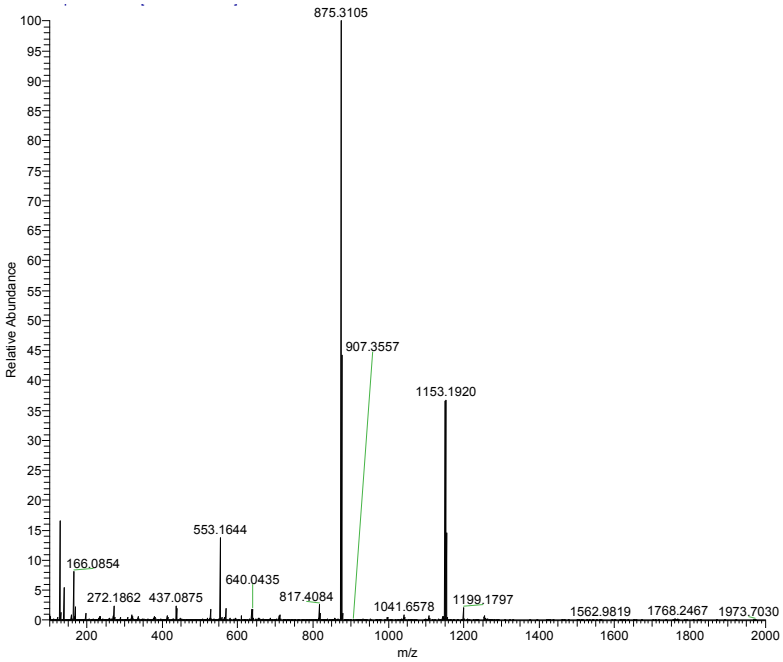

Figure S17. ESI-MS spectrum of **2d** (m/z 875). M/z 1153 corresponds to the $(NHC)_2Au_2Br$ species.

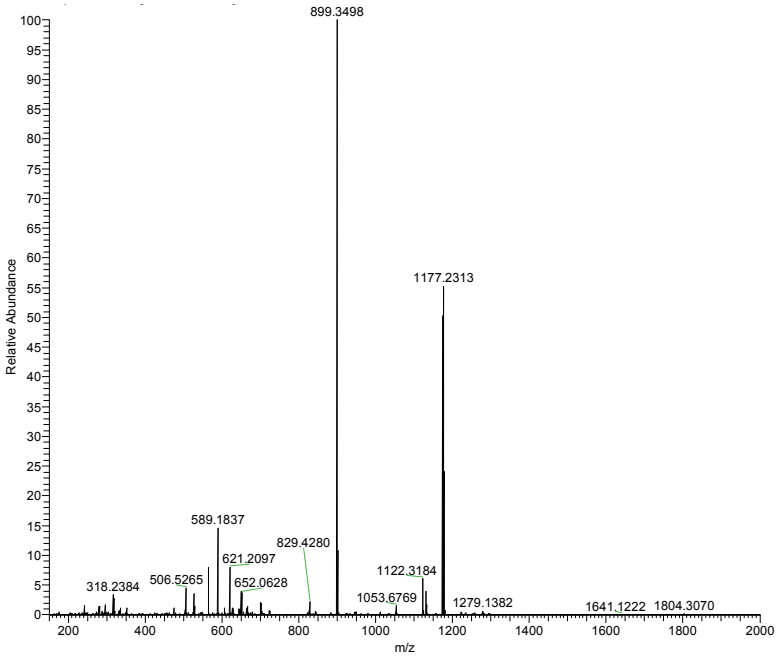

Figure S18. ESI-MS spectrum of **2e** (m/z 899). M/z 1177 corresponds to a cationic $(NHC)_2Au_2Br$ intermediate.

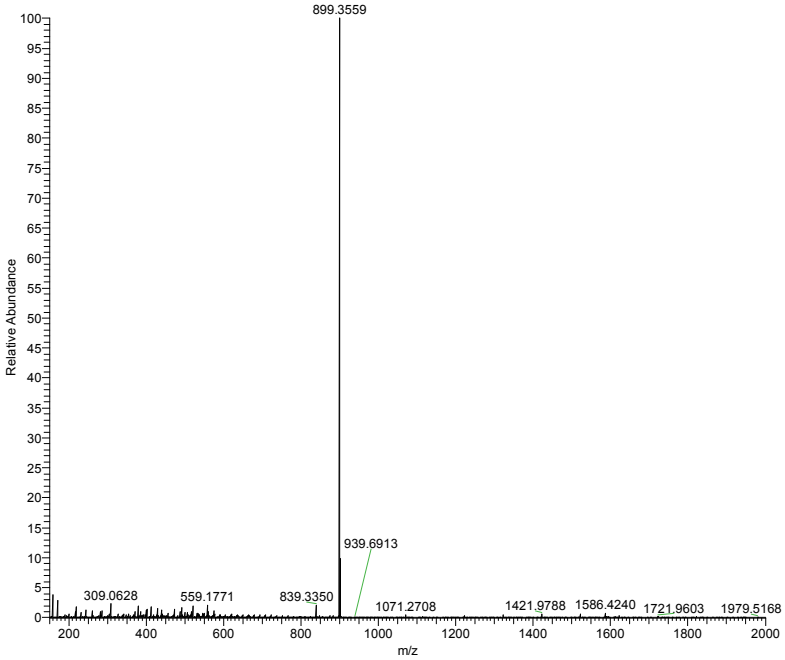

Figure S19. ESI-MS spectrum of **2f** (m/z 899).

1.5 HPLC analysis

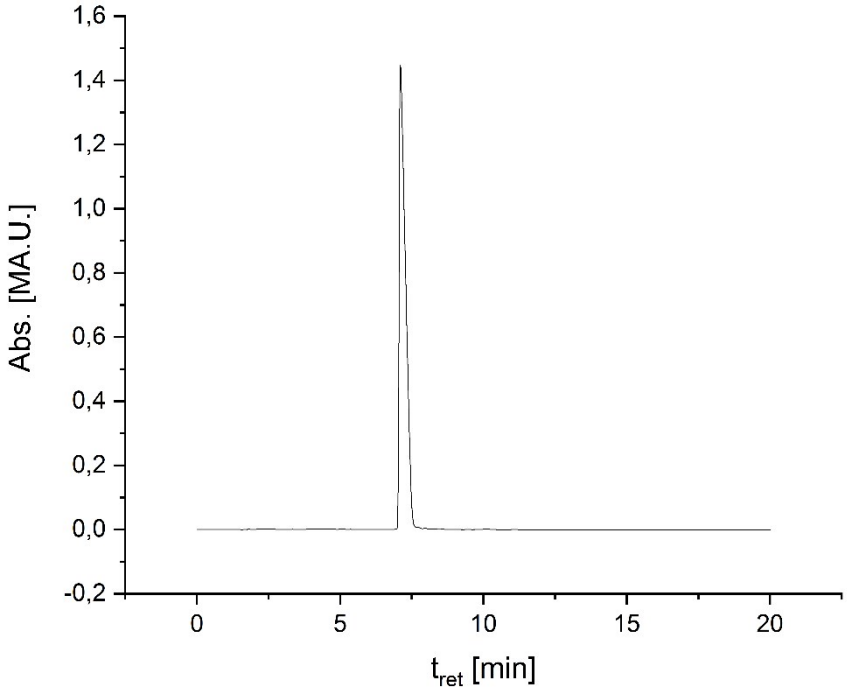

Figure S20. HPLC chromatogram of **2a** dissolved in ACN.

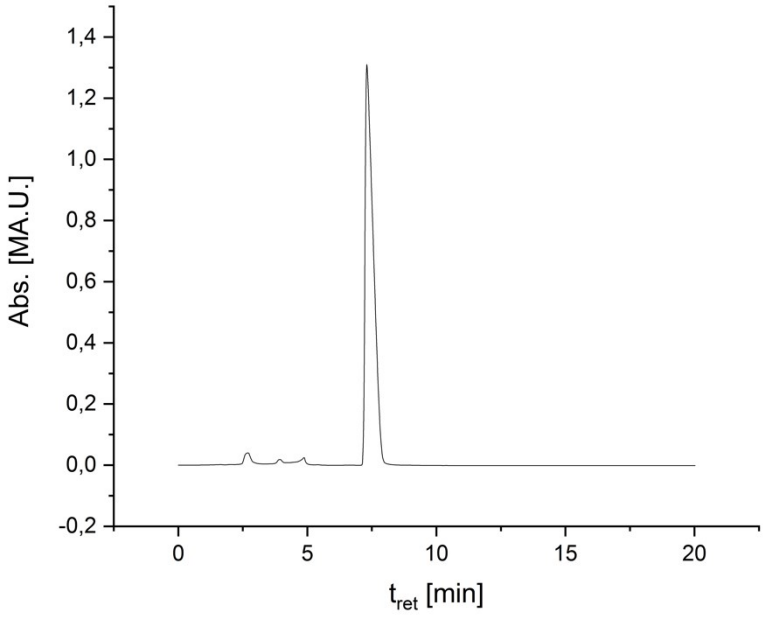

Figure S21. HPLC chromatogram of **2b** dissolved in ACN.

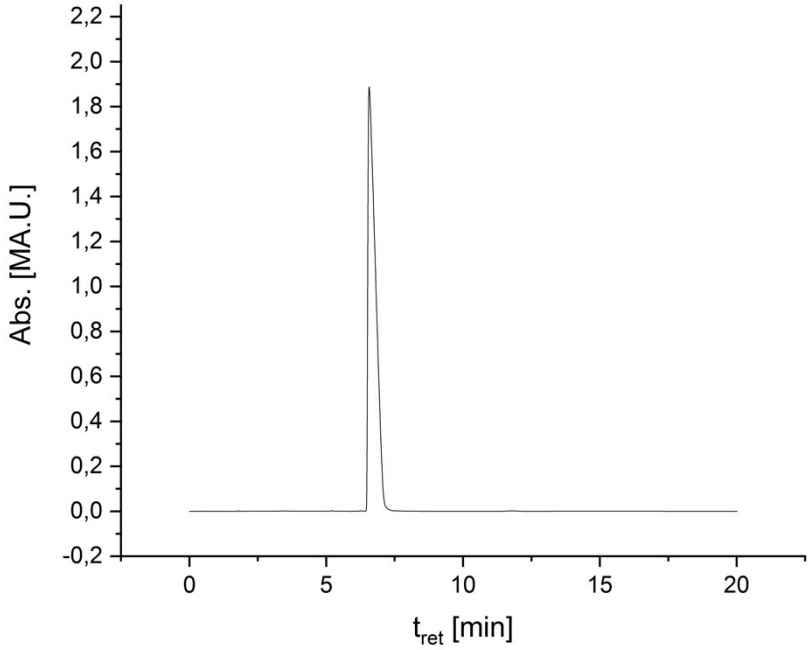

Figure S22. HPLC chromatogram of **2c** dissolved in ACN.

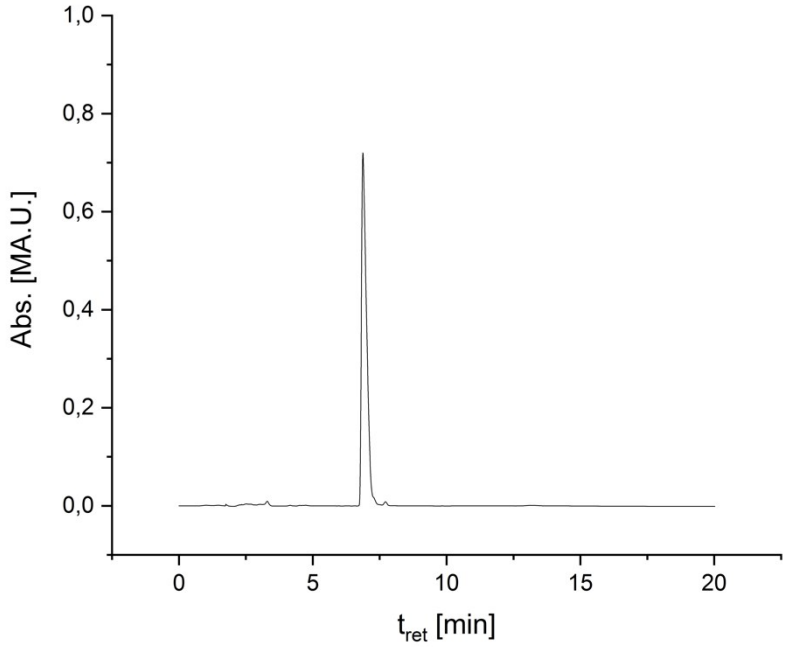

Figure S23. HPLC chromatogram of **2d** dissolved in ACN.

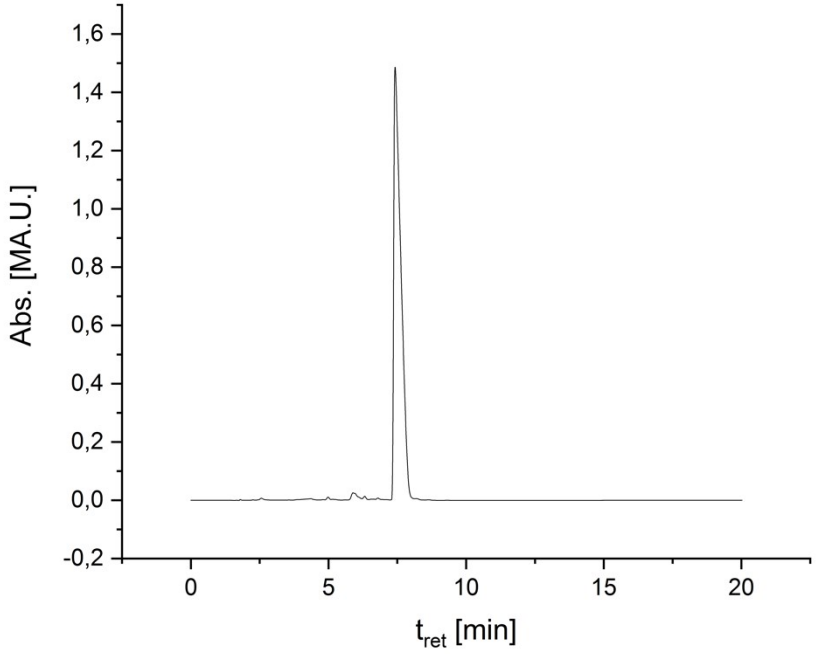

Figure S24. HPLC chromatogram of **2e** dissolved in ACN.

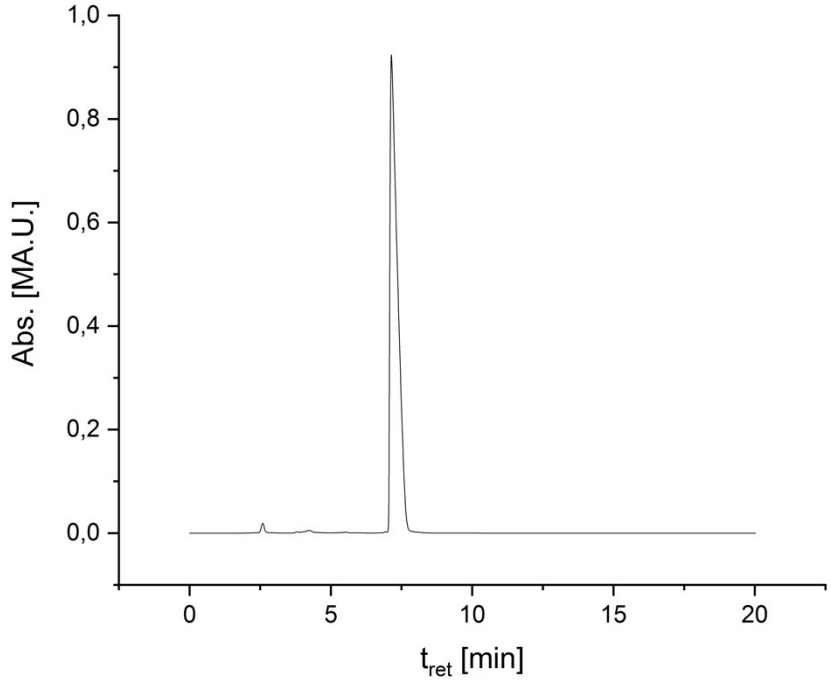

Figure S25. HPLC chromatogram of **2f** dissolved in ACN.

2. Biological activity

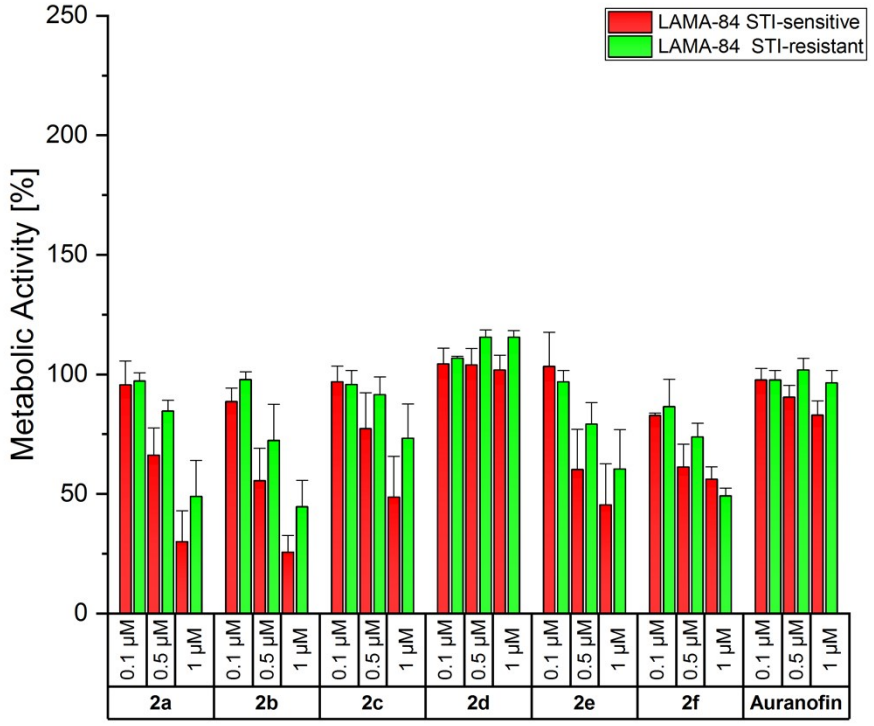

Figure S26. Anti-metabolic activity of complexes **2a-f** in comparison to Auranofin using different concentrations (0.1, 0.5 and 1 µM) in LAMA-84 STI-sensitive (red) and STI-resistant (green) cancer cells. The metabolic activity in the absence of the compounds was set at 100%. The mean + standard error was calculated from three independent experiments.

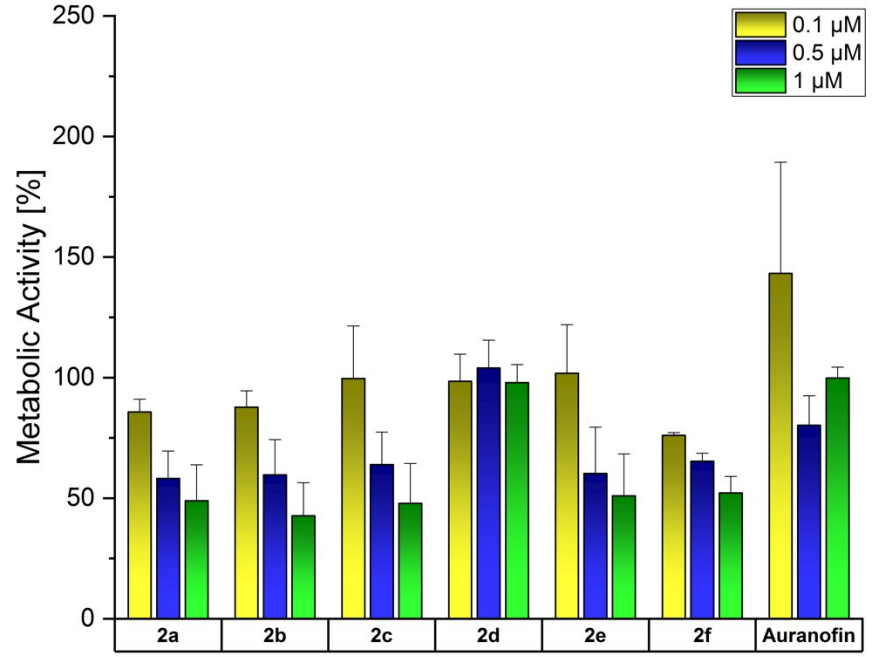

Figure S27. Anti-metabolic activity of complexes **2a-f** in comparison to Auranofin using different concentrations (0.1, 0.5 and 1 µM) in HL-60 cells. The metabolic activity in the absence of the compounds was set at 100%. The mean + standard error was calculated from three independent experiments.

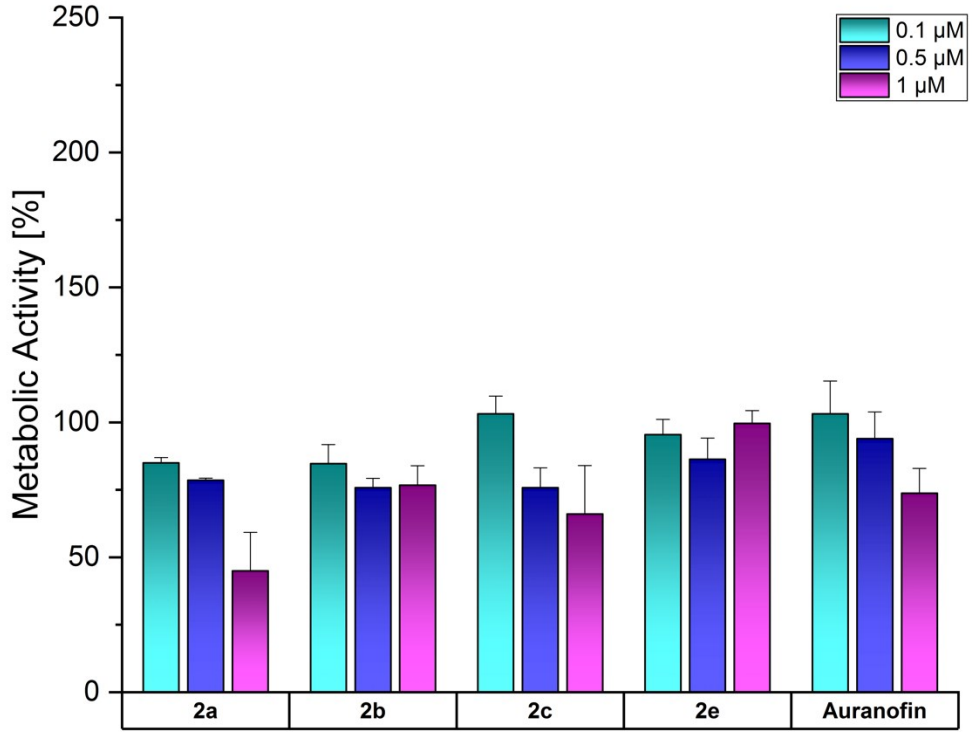

Figure S28. Anti-metabolic activity of complexes **2a-c**,**e** in comparison to Auranofin at different concentrations (0.1, 0.5 and 1 µM) in the non-cancerous lung fibroblast cell line SV-80. The metabolic activity in the absence of the compounds was set at 100%. The mean + standard error was calculated from three independent experiments.